Formation of Networked Microgrids for Operational Flexibility and Resilience

Marios Shimillas[1], Balaji V. Venkatasubramanian[2], Nikos Hatziargyriou[3], Mathaios Panteli[1]
[1]Department of Electrical and Computer Engineering, University of Cyprus, Nicosia, Cyprus
[2]School of Technology, Woxsen University, Telangana, India
[3]School of Electrical and Computer Engineering, National Technical University of Athens, Athens, Greece
[siimillas.marios, panteli.mathaios]@ucy.ac.cy;
balaji.venkateswaran@woxsen.edu.in;
nh@power.ece.ntua.gr

***Abstract*—In the evolving landscape of active distribution networks (DN), their resilience and reliability are of paramount importance, especially in the face of severe disturbances and climate-induced extreme weather. In this context, this paper introduces an approach to network reconfiguration that facilitates the formation of networked microgrids (NMGs) to enhance operational flexibility and resilience. The methodology incorporates radiality constraints, enabling dynamic modifications in the radial topology of the DN, while preventing the formation of loops or isolated buses in the reconfigured networks. It further accommodates diverse scenarios, including multiple line outages and limited distributed energy resources (DERs) including photovoltaics (PVs), battery energy storage systems (BESSs) and diesel generator (DG). The multi-temporal feature of the proposed methodology provides a clear quantification of the power imbalance in each microgrid (MG) and the operational status of DERs (e.g., BESS state of charge) over the simulated period. Case studies on a modified IEEE 33-bus system demonstrate the approach's effectiveness in dynamic resource management (BESS, PV) and in lowering the NMGs operational costs, including both DERs generation and load shedding costs.**

***Index Terms*—Resilience, Reliability, Network Reconfiguration, Microgrids, Renewable Energy, Distributed Generation**

I. Introduction

The rise of extreme weather events due to climate change has brought to light the fragility of current centralized electricity networks, which face growing reliability and resilience challenges. These challenges are accentuated as the networks reveal their vulnerabilities, struggling to withstand the increasing severity and frequency of such events, thereby elevating the risk of widespread outages. Furthermore, the significant increase in distributed renewable energy sources (RES) introduces additional complexity yet presents opportunities for enhancing network resilience [1]. This growing prevalence of decentralized RES necessitates a transition away from traditional centralized systems, compelling the energy sector to embrace these technologies and devise innovative solutions that enhance overall grid resilience and reliability.

In order to shift towards decentralized and distributed networks and mitigate the vulnerabilities of centralized electricity systems, much research has been conducted on utilizing microgrids (MGs) to enhance the resilience of power systems, especially for distribution networks (DNs), given their decentralized nature. Building on this foundation, the concept of networked microgrids (NMGs) progresses this idea by enabling several MGs to interconnect, thereby enhancing power sharing and greatly increasing the survivability of loads during extreme weather events. Reinforcing this concept, [2] and [3] have highlighted that MGs deliver enhanced technical and economic advantages when managed collectively at the community level, rather than functioning in isolation with distributed resources.

Previous studies, such as [4], have explored the potential of dividing DNs into multiple MGs to enhance reliability. In [5], a decentralized bi-level algorithm utilizing a linearized DistFlow model facilitates power exchange between the main grid and individual MGs. In [6], a consensus-based algorithm for power dispatch is outlined for the planning and operation of NMGs. In studies [7] and [8], researchers crafted a consensus-based strategy for dispatchable distributed energy resources (DERs), aiming for optimal supply sufficiency across each MG, and specifically tailored to operate within an emergency scheduling window of 2 to 4 hours, respectively.

While prior studies have advanced network reliability by integrating MGs with various strategic implementations, a considerable challenge persists in managing power imbalances during extended, large-scale emergency scenarios. Specifically, events spanning over a long-time horizon (e.g., a 24-hour emergency horizon) with extreme event scenarios present a critical gap, where inadequate management of these situations risks triggering widespread outages. Existing studies are limited in terms of investigating how MGs can effectively coordinate in such challenging contexts. Aiming to fill this gap, this paper introduces a NMG configuration strategy, enhancing resilience and optimizing operational costs for DERs and load shedding (LS) during operational emergencies, thereby mitigating their economic impact.

The aim of this work is to introduce an operational strategy for power system resilience, enabling the dynamic formation of NMGs to quantify potential power exchanges and enhance operational flexibility, especially in emergencies. This

This work was supported by the Horizon Europe program through the project "Reliability, Resilience and Defense Technology for the Grid" (R2D2) (Grant agreement ID: 101075714).

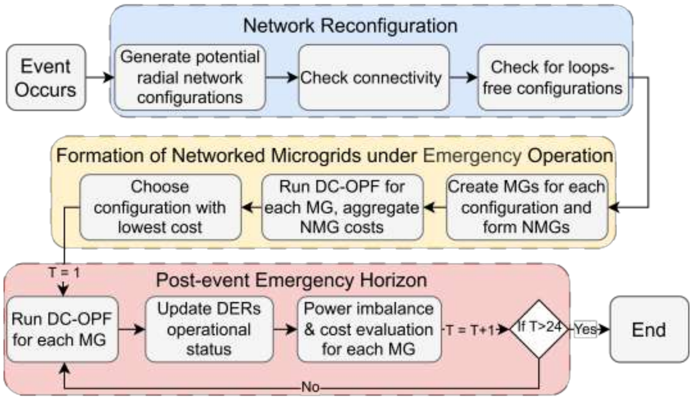

Fig. 1: Formation of NMGs under Emergency Operation

approach incorporates radiality, connectivity, and loop-free constraints to maintain a radial network topology during extreme events, ensuring the robustness of NMGs. Leveraging a multi-temporal framework, this methodology not only adeptly manages multiple line outages and DERs constraints but also precisely assesses the power imbalances within each MG and tracks the performance of DERs, such as the state of charge (SoC) for battery energy storage systems (BESSs), throughout the period of simulation. Through case studies on the modified IEEE 33-bus DN, the approach distinguishes itself by quantifying power exchange potentials between MGs and reducing operational costs in NMGs, including both DERs generation and LS expenses.

II. Methodology

This research outlines a framework for reconfiguring power networks by strategically establishing NMGs to strengthen operational flexibility and resilience in crisis situations within the DNs. As shown in Fig. 1, the suggested methodology can be described into three sequential steps: (A) Network Reconfiguration, (B) Formation of NMGs under Emergency Operation, (C) Post-event Emergency Horizon. Details of the proposed approach can be found hereafter.

A. Network Reconfiguration

Among the key aspects of the reconfiguration problem, radiality, connectivity and loop-free constraints are particularly significant [9], [10]. They are vital for quickly establishing a viable topology, key to strengthening the resilience and interconnectivity of NMGs, especially in the presence of extreme events.

In this context, the methodology initiates by identifying all possible reconfigurations that the network can embrace in the aftermath of multiple power line outages. It assesses the impact of extreme events on network line status from the outset, exploring all potential combinations based on the initially available open tie-lines (TLs), which exist within the network's configuration. This exploration, quantified as 2^n combinations where n represents the total number of TLs and the binary states indicate open (0) or closed (1) conditions, specifies the TL activations necessary to preserve the network's radial structure. Following the radiality principle $N_{lines} = N_{bus} - 1$, the approach ensures the active connection count N_{lines} is precisely one less than the bus count N_{bus}, a defining characteristic of radial networks.

Building upon the initial exploration of TLs (2^n), the methodology leverages sectionalizers at each bus to further enhance the reconfiguration possibilities. By sequentially activating TLs, the approach expands the feasible network configurations. This process maintains radiality constraints by progressively increasing the number of simultaneously opened line segments, starting with one and then moving to two, followed by subsequent increments, each time substituting the opened segments with an equivalent number of TLs. This iterative strategy continues until the total number of sections deactivated, whether due to faults or as part of the reconfiguration strategy, matches the number of TLs available. The comprehensive assessment of all potential radial reconfigurations is encapsulated by the combinatorial formula (1):

$$\sum_{f=N_{\mathrm{FL}}}^{N_{\mathrm{TL}}} C(N_{\mathrm{TL}}, f) \times C(N_{\mathrm{NFL}}, N_{\mathrm{NFL}} - (f - N_{\mathrm{FL}})) \quad (1)$$

which quantifies all possible radial network configurations by multiplying the number of combinations to activate TLs, $C(N_{\mathrm{TL}}, f)$, with the number of combinations that non-faulted lines are replaced by unused TLs due to sectionalizers operation, $C(N_{\mathrm{NFL}}, N_{\mathrm{NFL}} - (f - N_{\mathrm{FL}}))$. Here, N_{TL} denotes the total number of TLs, N_{FL} the number of faulted lines and N_{NFL} the non-faulted lines. The index f represents the number of TLs that can be closed to ensure network radiality. The term $(f - N_{\mathrm{FL}})$ provide the non-faulted lines to open, considering unused TLs to meet the radiality criterion.

Following this, each possible radial network configuration is represented in graph form. This representation facilitates the subsequent integrity checks. Specifically, each graph is checked for connectivity using Breadth-First Search (BFS), ensuring that every part of the network is reachable from any node [11]. Similarly, Depth-First Search (DFS) is employed to confirm acyclicity, which is essential to prevent the formation of loops within the network [12]. Ultimately, this process results in a set of viable network configurations that satisfy the stringent criteria of radiality, connectivity, and loop-free. Only those combinations where the network adheres to these essential conditions are considered further.

B. Formation of NMGs under Emergency Operation

The methodology's next step for NMG formation builds on the prior work detailed in the previous subsection, initiating with an evaluation of previously identified viable networks for MGs establishment, ensuring the presence of energy resources among the formed MGs. This approach prioritizes forming MGs based on RESs, starting with the strategic linkage of BESSs to proximate photovoltaic (PV) sources via a BFS algorithm. This strategy enhances energy management by effectively pairing storage with renewable sources. Following this, MGs systematically address intermediate and neighboring loads according to their capacity, aiming to cover as much network demand as feasible.

Conversely, existing stationary diesel generators (DG) are utilized into the MG configuration only after the renewable-based MGs have been established. This strategic sequencing underscores the role of DG as a secondary measure, designed to provide additional grid security and reliability, particularly in instances where renewable sources might be insufficient. Simultaneously, the process ensures that all loads are considered, and dynamically adjusts to accommodate unassigned loads. Through this approach, the methodology successfully reconfigures the network into a series of interconnected MGs, which can either stand alone or form NMGs.

After the establishment of MGs that interconnect to form NMGs, the methodology advances to the optimization phase, aiming to identify the most operationally cost-efficient configuration. This crucial step involves a DC-OPF approach, chosen for its computational efficiency in radial networks [13], with the objective function encapsulated by equation (2). It aims to minimize the operational expenses for each MG, including both DERs generation and LS costs, thereby enhancing the overall operational cost-efficiency of the NMG in a unified process. The objective function for each MG m, at time step t, can be found as:

$$\begin{aligned}\min\Bigg(&\sum_{g=1}^{N_{\text{DG}}} c_g \cdot P_{m,g,t}^{\text{DG}} + \sum_{p=1}^{N_{\text{PV}}} c_p \cdot P_{m,p,t}^{\text{PV}} + \\ &\sum_{b=1}^{N_{\text{BESS}}} \left(c_b^{\text{c}} \cdot P_{m,b,t}^{\text{BESS,c}} + c_b^{\text{d}} \cdot P_{m,b,t}^{\text{BESS,d}}\right) + \sum_{i=1}^{N_{\text{bus}}} c_i \cdot P_{m,i,t}^{\text{LS}}\Bigg), \\ &\forall m \in MG, \forall t \in T.\end{aligned} \tag{2}$$

where N_{DG}, N_{PV}, N_{BESS}, N_{bus} are the numbers of DGs, PVs, BESSs, and buses in turn, within each MG. $P_{m,g,t}^{\text{DG}}$ and $P_{m,p,t}^{\text{PV}}$ denote the power generated by DG g and PV p, with costs c_g and c_p, respectively. $P_{m,b,t}^{\text{BESS,c}}$ and $P_{m,b,t}^{\text{BESS,d}}$ represent the charging and discharging actions of BESS b, with c_b^c and c_b^d as the associated costs. $P_{m,i,t}^{\text{LS}}$ refers to the LS at bus i, with c_i being the cost factor associated with LS at each bus. Upon concluding the optimization for the event time, the algorithm identifies the most operationally cost-efficient option among the viable NMG configurations generated in the previous step in Section II.A and then progresses to the subsequent phase.

C. Post-event Emergency Horizon

Upon identifying the most cost-effective network configuration to establish NMGs, the algorithm proceeds to a post-event emergency horizon, spanning a 24-hour period following the initial event, segmented into hourly intervals. This approach leverages DERs to significantly reduce LS during this period, aiming for the greatest feasible reduction. It conducts a comprehensive simulation to identify which operational strategies most effectively utilize resources at different times to best mitigate extreme event impacts, as shown in Section III.

During these intervals, the objective as outlined in equation (2) is to minimize the operational costs of each MG through the DC-OPF, resulting in the overall cost for the NMGs. The multi-temporal aspect of this methodology provides a detailed evaluation of active power imbalance within each MG, and simultaneously within the NMG, by accounting for all potential active power exchanges between MGs. It also tracks the operational status of DERs, such as the SoC of BESS throughout the simulation period. The equation representing the power imbalance j in each MG m, at any given time step t is detailed as follows:

$$\begin{aligned}P_{m,j,t}^{im} =& \sum_{g=1}^{N_{\text{DG}}} P_{m,g,t}^{\text{DG}} + \sum_{p=1}^{N_{\text{PV}}} P_{m,p,t}^{\text{PV}} - \sum_{b=1}^{N_{\text{BESS}}} (P_{m,b,t}^{\text{BESS,c}} - P_{m,b,t}^{\text{BESS,d}}) \\ &- \sum_{i=1}^{N_{\text{bus}}} (P_{m,i,t}^{\text{d}} - P_{m,i,t}^{\text{LS}}), \forall m \in MG,\ \forall t \in T\end{aligned} \tag{3}$$

where $P_{m,i,t}^{d}$ is the total active load being served by MG m at time t. This equation assesses the capability for power exchange among MGs by quantifying the surplus or shortage of power in each MG at any given time.

In scenarios where PV generation drops during peak hours, this methodology ensures each MG relies on its BESS until the SoC reaches the minimum limit, supplemented by power exchanges from MGs with available DG. In extreme cases, increasing LS may be necessary to maintain network stability and resilience.

III. Case Studies

To assess the effectiveness of the proposed methodology of forming NMGs under emergency operation as outlined in Section II, a modified IEEE 33-bus DN, incorporating PVs, BESSs, and a DG was employed, as illustrated in Fig. 2a. The peak load of this network reaches 3,715 MW. All case studies were conducted using an Intel i7-1360P processor at 2.20 GHz with 16GB of RAM.

To simulate real-world conditions and evaluate resilience against extreme events, multiple line outages were considered, including the faulting of 4 lines (6-7, 9-10, 23-24, 30-31) and the grid's failure to provide power to the study network. Normalized solar irradiation and load profiles, as well as the technical information of DERs used in the evaluation, are illustrated in Fig. 3 and detailed in Tables I (DG, PV) and II (BESS), respectively. Notably, each BESS is capable of being fully charged or discharged within six time steps, and it is posited that they begin from a fully charged state. The penalty factor of LS is set to 225 \$/MW [14].

Following the methodology outlined in Section II.A., the process identified 33 possible radial network configurations for forming NMGs. Among these, only three configurations satisfied the essential criteria of ensuring full connectivity, loop avoidance and radiality, marking them as suitable for establishing NMGs. In each of these viable configurations, 7 MGs emerged, each equipped with a BESS and one PV unit, except for the final MG, which exclusively relies on a DG located in bus 1. To establish these MGs, TLs 1, 3, 4, and 5 were closed, while lines 2-19, 4-5, 13-14, 16-17, 21-22, and 28-29 were opened, as Fig.2b shows.

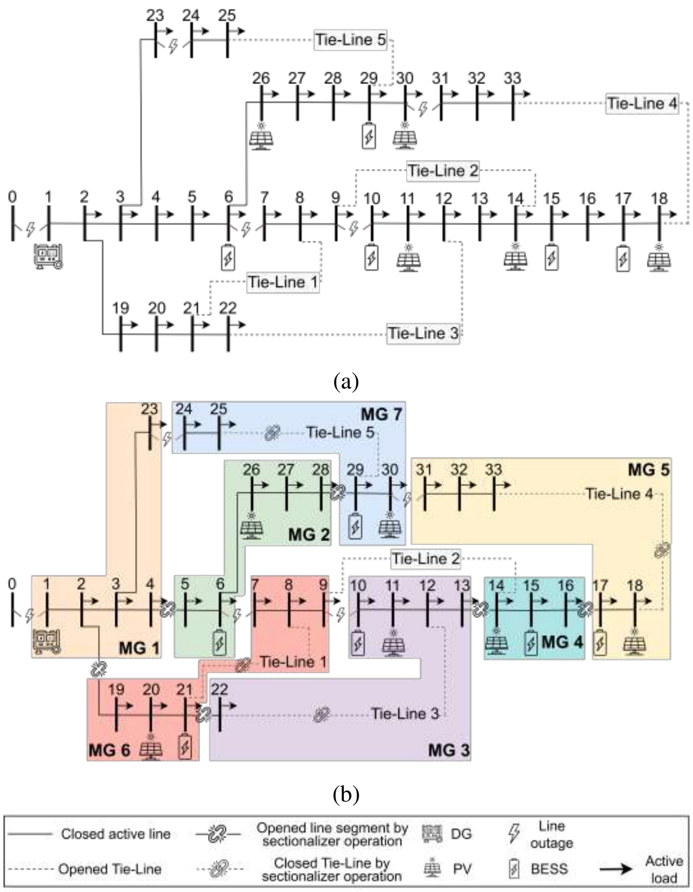

Fig. 2: Modified IEEE 33-bus distribution network: (a) Base Case Scenario (b) Formation of NMGs under Emergency Operation.

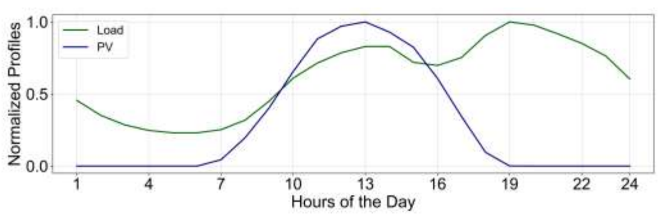

Fig. 3: Load and PV profiles.

The initial costs for the three viable network configurations were 305.5 \$, 305.4 \$, and 307.4 \$, determined from the objective function (2) for DERs and LS costs at the initial time step. Given the identical cost performance between these options, the second configuration was chosen for demonstration of the post-event emergency horizon, as illustrated in Fig.2b.

A. Case Study I: Base Case Scenario

This subsection presents the optimization outcomes from the scenario without the proposed methodology. Fig. 4 displays the network's power imbalance results after the event occurs with the faulted lines being the same for all the scenarios as described before. The depicted figure distinctly illustrates the network's inability to meet load demands throughout the entire duration, highlighting the critical need for implementing robust strategies to ensure resilience and reliability in power supply. Especially in DNs, integrating such measures is of paramount importance for mitigating the compounded challenges brought on by extreme weather events.

TABLE I: DG & PV technical informations

Bus	Pmax (MW)	Type	Costs (\$/kWh) [15]
1	0.9	DG	0.13
11	0.6	PV	0.05
14	0.6	PV	0.05
18	0.6	PV	0.05
20	0.9	PV	0.05
26	1.2	PV	0.05
30	1.6	PV	0.05

TABLE II: BESS technical informations

Bus	SoC (MWh)		n_{ch}/n_{dis}	SoC rate	Costs (\$/kWh) [15]	
	min	max	(%)	(MWh)	Charge	Discharge
6	0.07	0.7	90	0.105	0.09	0.15
10	0.07	0.7	90	0.105	0.09	0.15
15	0.07	0.7	90	0.105	0.09	0.15
17	0.09	0.9	90	0.135	0.09	0.15
21	0.10	1.0	90	0.150	0.09	0.15
29	0.12	1.2	90	0.180	0.09	0.15

B. Case Study II: Formation of NMGs under Emergency Operation

In this case study, the proposed formation of NMGs for operational flexibility and resilience is applied. Fig. 5 graphically depicts the power imbalance for two of the seven MGs formed. The figures showcase the results for MG 1 (Fig.5a), which utilizes a DG, and for MG 4 (Fig.5b), which is equipped with a BESS and a PV system. It is noted that MG 4 shares similar graphical patterns with the other five MGs (MGs 2-3 and 5-7), demonstrating variations in LS, with some MGs (5-7) experiencing more LS and others (MGs 2-4) experiencing less throughout the emergency horizon.

In the power imbalance analysis, MG 1 consistently shows a surplus throughout all hours, attributable to the constant output from the DG within MG 1 that exceeds the demand. MG 4 experiences a transition from surplus to shortage starting at hour 18, except for an initial minor shortage, demonstrating surplus power production during the day. In contrast, during the evening, the inability to generate PV power leads to a shortfall in meeting increased demand. Consequently, only a portion of the total load is supported from the presence of BESS. Meanwhile, MGs 5-7 face a distinct challenge, experiencing more pronounced LS during morning hours than MG 4. This is mainly due to their limited capacity to meet

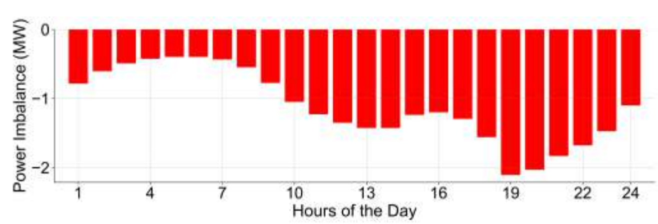

Fig. 4: Power imbalance over post-event emergency horizon for Case Study I - Base Case Scenario

(a)

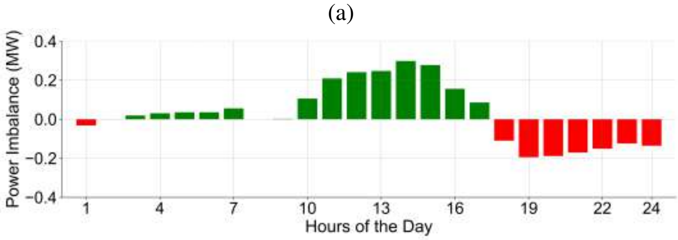

(b)

Fig. 5: Power imbalance over post-event emergency horizon for Case Study II - Formation of NMGs under Emergency Operation: (a) MG 1, (b) MG 4.

(a)

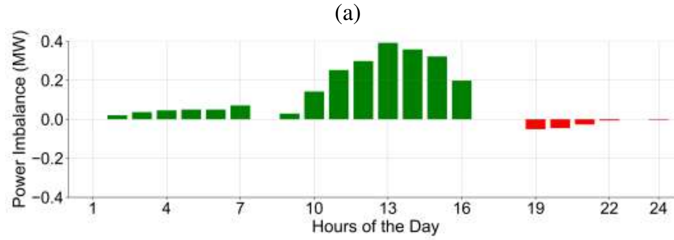

(b)

Fig. 6: Power imbalance over post-event emergency horizon for Case Study III - Formation of NMGs under Emergency Operation with Power Exchanges: (a) MG 1, (b) MG 4.

early demand spikes, as their power generation and storage discharge are not sufficient to handle the increased load.

Comparing the base scenario with Case Study II, the former struggles with continuous power shortages, underscoring the need for strategies to improve reliability. In contrast, the proposed approach exhibits mixed performance: while MG 1 consistently exceeds demand due to stable output, MG 4 (as well as MGs 2-3 and 5-7) faces dynamic power imbalances, reflecting the complexities of balancing production and consumption under extreme conditions. Alongside, there's a 33.5% overall reduction in LS relative to the baseline scenario, showcasing the potential of NMGs for improved flexibility and resilience, despite challenges during peak demand periods.

The computational time of the proposed approach is evident in the processing times: network reconfiguration was completed in 0.17 seconds, formation of NMGs under emergency operation in 1.34 seconds, and post-event emergency horizon analysis with all 24 hourly steps completed in 12.54 seconds. These findings highlights the computational time of the proposed approach over the entire 24-hour simulation period in the example.

C. Case Study III: Formation of NMGs under Emergency Operation with Power Exchanges

In the enhanced scenario of Case Study III, the proposed methodology incorporates the aspect of potential power exchanges, achieving a 57.5% reduction in LS across the entire emergency horizon compared to Case I, significantly enhancing system resilience and reliability. In particular, the power imbalances for the selected MGs (1 and 4) are reevaluated in this context, as illustrated in Fig.6.

The MG 1 consistently shows a surplus of power at all times, thanks to the stable performance of the DG. Specifically, at the onset of the observation period, and from 18 to 24 hours when PVs are not contributing, MG 1 performs a supportive role by exporting power surplus to neighboring MGs undergoing LS. This is depicted in Fig. 6a, where there is a zero balance due to the exchange of its surplus. Moreover, MGs 5-7, which previously experienced power shortages at certain times, now have the opportunity to mitigate these shortfalls by receiving power from MG 4 (likewise from MGs 2,3) during hours 7 to 9, and again at hour 17, specifically from a surplus generated by their PV. In instances where the surplus from MGs 2-7 is not sufficient, MG 1 steps in by contributing its surplus to cover any unmet demand, ensuring a stable supply across the network for these times, as verified by the Figs.6a, 6b. The surplus power available in MG 4 during the hours of 2 to 7 and at 9 originates from the surplus discharge of BESS.

Notably, between the hours of 10 and 16, the network attains a state of self-sufficiency, with each MG independently meeting its energy requirements, mirroring the surplus observed in Case II. This period highlights the system's capability for self-management, attributed to power generated by PV systems.

D. Case Study IV: Cost Evaluation

Following the discussion of the network's power imbalance, the subsequent analysis in Table III, presents a cost comparison among the three case studies. Case II indicates a substantial cost reduction, achieving 11.4% savings during morning hours, 5 and 6, compared to Case I. Savings peak for the 9 to 17 time steps with a maximumn reduction rate of 53.4%. On the contrary, from times 18 to 24, the methodology struggles, peaking at a 14.6% burden by time 24. However, when considering the enhanced capabilities of NMGs to engage in power exchanges, the cost savings profile is significantly improved, as indicated by Case III results. This leads to over 53.4% savings from time 1 to 17, demonstrating the benefits of energy sharing. Although there is a notable decrease in savings towards the end of the day, from time 18 to 20 and 22, 24, the cost reduction remains positive, with the lowest but crucial 0.4% saving observed at time 24, indicating the

TABLE III: Cost Comparison for Cases Studies

Time	Case I Cost ($)	Case II Cost ($)	Case III Cost ($)	Cost reduction on Case II (%)	Cost reduction on Case III (%)
1	300.4	305.4	237.2	-1.7	21.0
2	231.6	223.6	185.0	3.5	20.1
3	188.2	174.8	152.2	7.1	19.1
4	162.9	146.5	132.9	10.0	18.4
5	152.0	134.7	124.6	11.4	18.0
6	152.0	134.7	124.6	11.4	18.0
7	145.3	140.0	107.8	3.6	25.8
8	189.9	122.2	103.6	35.6	45.4
9	247.2	166.1	162.8	32.8	34.1
10	324.8	228.9	228.9	29.5	29.5
11	375.6	262.8	262.8	30.0	30.0
12	397.7	279.5	279.5	29.7	29.7
13	403.8	260.9	260.9	35.4	35.4
14	403.8	244.0	244.0	39.6	39.6
15	350.4	204.9	204.9	41.5	41.5
16	339.7	158.3	158.3	53.4	53.4
17	399.9	269.3	221.9	32.7	44.5
18	551.6	572.9	521.8	-3.9	5.4
19	696.8	738.4	690.9	-6.0	0.8
20	679.4	721.8	673.5	-6.3	0.9
21	630.7	681.9	631.3	-8.1	-0.1
22	582.4	631.0	577.9	-8.3	0.8
23	518.1	578.6	522.1	-11.7	-0.8
24	416.1	476.8	414.2	-14.6	0.4
Total	**8840.1**	**7858.2**	**6407.5**	**11.1**	**18.3**

resilience of the system even during periods of high demand. At times 21 and 23, there is a noted decrease of 0.1% and 0.8% respectively, suggesting that Case I stands out as the most operationally cost-effective and efficient solution for this particular time steps.

Taking into account the full span of the time horizon under consideration, the comprehensive analysis reveals that Case II achieves a total cost reduction of 11.1%, compared to Case I. Meanwhile, Case III demonstrates a substantial 18.3% decrease in costs relative to Case I, marking a significant enhancement in cost efficiency.

IV. Conclusions

In conclusion, this approach to network reconfiguration, enabling the formation of NMGs based on DERs, demonstrates significant potential in enhancing operational flexibility and resilience in DNs. Case studies on a modified IEEE 33-bus DN highlight the effectiveness of the proposed approach in addressing challenges posed by extreme events and power line outages, ensuring reliable power supply and optimizing operational costs associated with DERs and LS costs.

Notably, the case studies underscore the benefits of the proposed approach, with a significant 33.5% reduction in LS during the emergency horizon, with further reductions reaching 57.5% in Case Study III due to potential power exchanges among MGs. This enhancement significantly increases the resilience and reliability of the power DN. Economic analyses reveal marked cost savings, with reductions of 11.1% in Case Study II and 18.3% in Case Study III compared to Case Study I, highlighting the efficiency of the proposed energy management and resource sharing among NMGs.

Building on these findings, the results advocate for a dynamic and adaptive approach to network reconfiguration subject to the permissible switching actions in the DN: applying Case III's methodology during hours 1 to 20, and 22, 24, and restoring the network's initial configuration (Case I) at hours 21 and 23, thus offering a more economically viable alternative. It is worth noting here that for hours 10 to 16 the same cost reductions are observed for Cases III and II, as the MGs stand alone without needing support.

Future work will focus on evaluating the stochastic and dynamic behaviour of PV output variability and demand fluctuations, particularly during the switching actions of network reconfiguration. Additionally, the economic analysis will be extended to include the investment costs of sectionalizers, exploring the trade-off between sectionalizer use and LS. AC OPF models will also be employed to better capture technical parameters, such as voltage level of buses and system losses, providing a comprehensive evaluation of the proposed strategy.

References

[1] P. Mancarella and F. Billimoria, "The fragile grid: The physics and economics of security services in low-carbon power systems," *IEEE Power and Energy Magazine*, vol. 19, no. 2, pp. 79–88, 2021.

[2] P. Mancarella, G. Andersson, J. Peças-Lopes, and K. Bell, "Modelling of integrated multi-energy systems: Drivers, requirements, and opportunities," in *2016 Power Systems Computation Conference (PSCC)*, 2016.

[3] G. Liu, T. Ollis, M. Ferrari, A. Sundararajan, and K. Tomsovic, "Robust scheduling of networked microgrids for economics and resilience improvement," *Energies*, vol. 15, p. 2249, 03 2022.

[4] S. A. Arefifar, Y. Mohamed, and T. H.M. El-Fouly, "Optimum microgrid design for enhancing reliability and supply-security," *Smart Grid, IEEE Transactions on*, 09 2013.

[5] Z. Wang, B. Chen, J. Wang, and J. Kim, "Decentralized energy management system for networked microgrids in grid-connected and islanded modes," *IEEE Transactions on Smart Grid*, 06 2015.

[6] Z. Liu, Y. Yi, J. Yang, W. Tang, Y.-J. Zhang, X. Xie, and T. Ji, "Optimal planning and operation of dispatchable active power resources for islanded multi-microgrids under multi-agent consensus algorithm framework," *IET Generation, Transmission & Distribution*, 12 2019.

[7] A. Hussain, V.-H. Bui, and H.-M. Kim, "Resilience-oriented optimal operation of networked hybrid microgrids," *IEEE Transactions on Smart Grid*, no. 1, 2019.

[8] Z. Wang, B. Chen, J. Wang, and C. Chen, "Networked microgrids for self-healing power systems," *IEEE Transactions on Smart Grid*, 06 2015.

[9] M. Mahdavi, H. H. Alhelou, P. Gopi, and N. Hosseinzadeh, "Importance of radiality constraints formulation in reconfiguration problems," *IEEE Systems Journal*, no. 4, 2023.

[10] B. Wang, H. Zhu, H. Xu, Y. Bao, and H. Di, "Distribution network reconfiguration based on noisynet deep q-learning network," *IEEE Access*, vol. PP, pp. 1–1, 06 2021.

[11] A. Bundy and L. A. Wallen, *Breadth-First Search*. Springer Berlin Heidelberg, 1984.

[12] R. Tarjan, "Depth-first search and linear graph algorithms," in *12th Annual Symposium on Switching and Automata Theory*, 1971.

[13] B. V. Venkatasubramanian, M. Lotfi, M. Panteli, M. S. Javadi, and L. M. Carvalho, "Scalability analysis of convex relaxation methods for branch flow ac optimal power flow," in *2022 IEEE International Conference on Environment and Electrical Engineering and 2022 IEEE Industrial and Commercial Power Systems Europe (EEEIC / I&CPS Europe)*, 2022.

[14] A. Hussain, V.-H. Bui, and H.-M. Kim, "Optimal operation of hybrid microgrids for enhancing resiliency considering feasible islanding and survivability," *IET Renewable Power Generation*, 02 2017.

[15] A. Abdolahi, J. Salehi, F. Samadi Gazijahani, and A. Safari, "Probabilistic multi-objective arbitrage of dispersed energy storage systems for optimal congestion management of active distribution networks including solar/wind/chp hybrid energy system," *Journal of Renewable and Sustainable Energy*, 08 2018.